BN-Isosteres of Nonacene with Antiaromatic B_2C_4 and N_2C_4 Heterocycles: Synthesis and Strong Luminescence

Cheng Chen,[a] Zhi-Dong Chang,[a] Yong-Kang Guo,[a] Yan-Bo Huang,[a] and Xiao-Ye Wang[a,b]*

[a] C. Chen, Z.-D. Chang, Y.-K. Guo, Y.-B. Huang, Prof. Dr. X.-Y. Wang
State Key Laboratory of Elemento-Organic Chemistry, Frontiers Science Center for New Organic Matter, College of Chemistry, Nankai University, 300071 Tianjin, China
E-mail: xiaoye.wang@nankai.edu.cn

[b] Prof. Dr. X.-Y. Wang
State Key Laboratory of Luminescent Materials and Devices, South China University of Technology, 510640 Guangzhou, China

Abstract: Embedding both boron and nitrogen into the backbone of acenes to generate their isoelectronic structures has significantly enriched the acene chemistry to offer appealing properties. However, only small BN-heteroacenes have been extensively investigated, with BN-embedded heptacenes as the hitherto longest BN-acenes. Herein, we report the synthesis of three new nonacene BN-isosteres via incorporating antiaromatic 1,4-dihydro-1,4-diborinine (B_2C_4) and 1,4-dihydropyrazine (N_2C_4) heterocycles. These BN-nonacenes represent a new length record in the field of BN-heteroacenes. The position of the boron- and nitrogen-embedded antiaromatic rings manifests substantial influence on the molecular orbital arrangement, and consequently, the radiative transition rate of **BN-3** is greatly enhanced compared with **BN-1** and **BN-2**, realizing a high fluorescence quantum yield of 92%. This work provides a novel design concept of BN-heteroacenes and reveals the importance of precisely BN-doping.

Acenes are a unique class of polycyclic aromatic hydrocarbons (PAHs) with linearly fused benzene rings (Figure 1a). They have served as high-efficiency luminescent materials (e.g. anthracene) and high-mobility organic semiconductors (e.g. pentacene), thus attracting enormous attention from organic chemists and materials scientists.[1] However, the synthesis of acenes longer than pentacene (the number of fused benzene rings $N > 5$, referred to as large acenes) has remained a huge challenge owing to their high instability under the ambient conditions.[2] Several strategies have been proposed to deal with this problem. For example, the on-surface synthesis under ultrahigh vacuum and the polymer-matrix-assisted synthesis in the solid state have enabled the construction of large acenes up to dodecacene ($N = 12$),[3] and very recently, polyacene has even been achieved by using metal–organic frameworks as the reaction host.[4] In sharp contrast, large acenes synthesized via the traditional wet chemistry have still been limited to nonacene ($N = 9$).[5]

On the other hand, constructing the isoelectronic structure of acenes by embedding heteroatoms (e.g. B, N, O, and S) into the backbone provides a viable way to develop acene-based functional materials.[6] Nevertheless, many of the reported heteroacenes have unequal valence electrons to their all-carbon skeletons,[7] and thus the reductive/oxidative reactions have to be utilized to achieve the isoelectronic structure of acenes in the charged state.[8] Considering the rapid development of BN-doped PAHs in recent years,[9] embedding the same number of B and N atoms in acenes can afford novel acene BN-isosteres in the neutral form. To date, only short BN-heteroacenes (e.g. BN-anthracenes) have been widely studied, showing intriguing optoelectronic properties,[10] whereas BN-isosteres of large acenes have been rarely reported, with BN-heptacene ($N = 7$) as the hitherto longest backbone.[11]

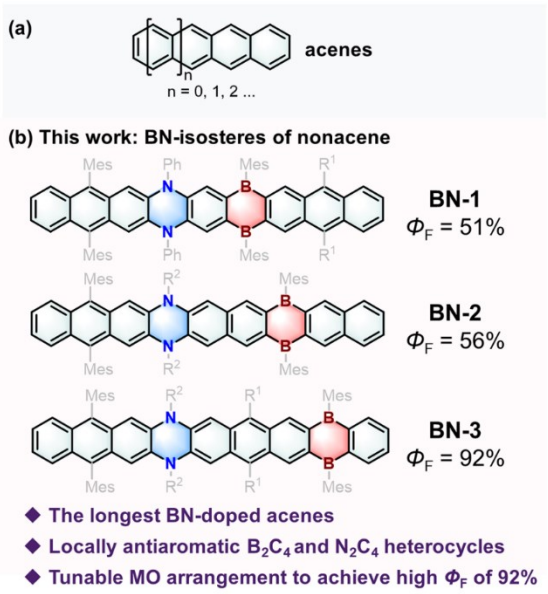

Figure 1. (a) Structural illustration of acenes. (b) Chemical structures of BN-doped nonacenes **BN-1**, **BN-2**, and **BN-3** reported in this work. Mes = 2,4,6- trimethylphenyl; R^1 = 3,5-(diisopropyl)phenyl; R^2 = 4-*tert*-butylphenyl. MO: molecular orbital. Φ_F: fluorescence quantum yield.

Herein, we report the synthesis of three BN-isosteres of nonacene as the new length record for BN-doped acenes, including **BN-1**, **BN2**, and **BN-3** (Figure 1b). In these compounds, 4π-antiaromatic 1,4-dihydro-1,4-diborinine (B_2C_4) and 8π-antiaromatic 1,4-dihydropyrazine (N_2C_4) heterocycles are embedded in the nonacene backbone. The position of the B_2C_4 and N_2C_4 rings shows significant impact on the molecular orbital arrangement, endowing **BN-3** with a favorable radiative transition and thus a high fluorescence quantum yield (Φ_F) of 92%. This work provides a new type of large acene BN-isosteres and illustrates the important role of precisely doping of acenes with boron- and nitrogen-based antiaromatic rings.

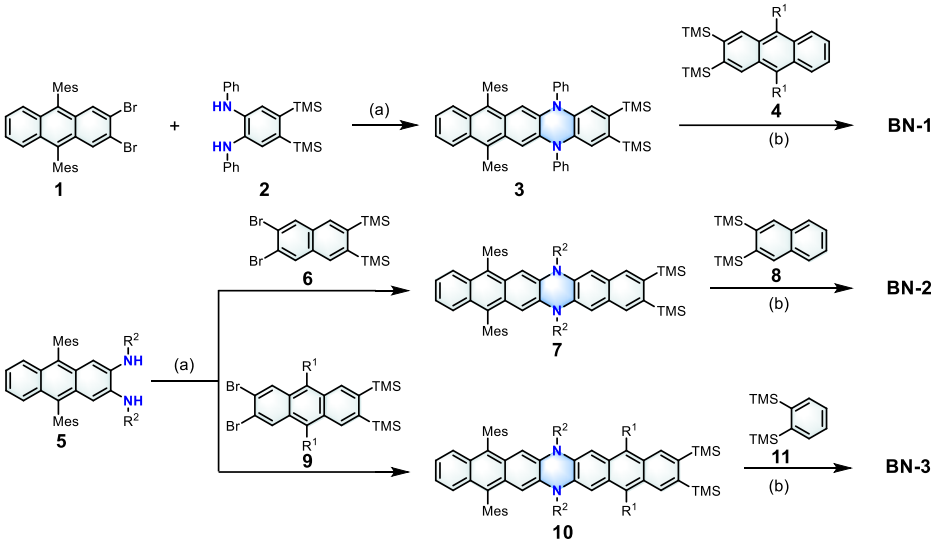

Scheme 1. Synthetic route to the BN-isosteres of nonacene. Reagents and conditions: (a) $Pd(dba)_2$, P*t*-Bu_3•HBF_4, *t*-BuONa, toluene, 110–120 °C, 18–24 h. Yields: 52% for **3**, 30% for **7**, and 66% for **10**. (b) i) BBr_3, heptane, 120 °C, 48 h; ii) MesMgBr, toluene, 0 °C to rt,18 h. Two-step yields: 6% for **BN-1**, 27% for **BN-2**, and 35% for **BN-3**. R^1 = 3,5-(diisopropyl)phenyl; R^2 = 4-*tert*-butylphenyl.

Synthetic routes to **BN-1**, **BN-2**, and **BN-3** are depicted in Scheme 1. First, Buchwald–Hartwig coupling reactions were employed to construct bis(trimethylsilyl)-substituted dihydrodiazaacenes **3**, **7**, and **10** in 30–66% yields. Then these N-doped acenes were treated with bis(trimethylsilyl)-functionalized arenes (**4**, **8**, or **11**) in the presence of boron tribromide (BBr_3) to form BN-doped nonacene backbones via the Si/B exchange cross-annelation reaction. Finally, the bulky mesityl (Mes) moieties were introduced via a nucleophilic substitution reaction, giving **BN-1** in 6%, **BN-2** in 27%, and **BN-3** in 35% yields for two steps. A 1 : 3 ratio of the two bis(trimethylsilyl)-substituted precursors was utilized to suppress the Si/B exchange homo-annelation, and thus the dihydrodiboraacenes and the N_4B_2-doped acenes were not observed. The target BN-doped nonacenes were characterized by ^1H and ^{13}C NMR spectroscopies as well as high-resolution mass spectrometry (HRMS). Moreover, their solids stored under air were highly stable for at least six months. The excellent stability of the title compounds was also demonstrated by monitoring their ^1H NMR spectra in solutions, with no obvious changes observed for one week.

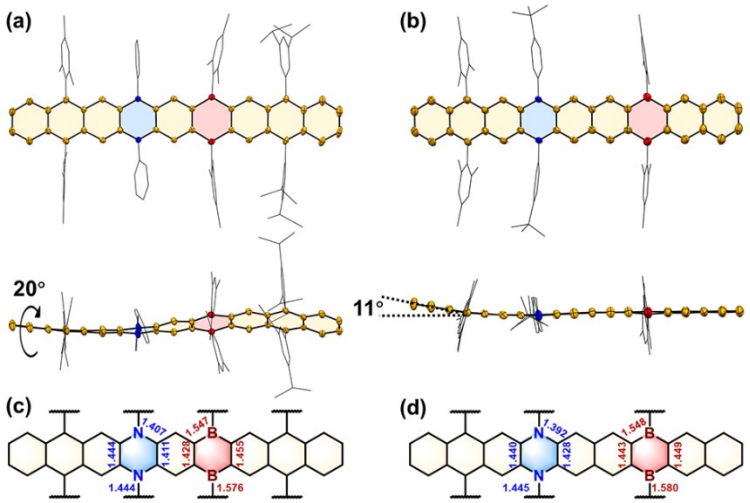

Figure 2. (a–b) Single-crystal structures of **BN-1** and **BN-2** showing their top and side views. The twisting angle in **BN-1** and the bending angle in **BN-2** are defined as the dihedral angle between the central and the terminal benzene rings. Thermal ellipsoids are shown at 50% probability. Hydrogen atoms are omitted for clarity. (c–d) Selected bond lengths of **BN-1** and **BN-2**.

Single crystals of **BN-1** and **BN-2** suitable for X-ray structural analysis were successfully obtained via slowly diffusing *n*-hexane into their dichloroethane solutions (Figure 2).[12] Unfortunately, the growth of high-quality single crystals of **BN-3** was difficult, and the obtained crystals always contained disordered solvents within the unit cells. Therefore, the structural characters of **BN-1** and **BN-2** were analyzed in detail. **BN-1** exhibits a twisted backbone with a twisting angle of 20°, while the skeleton of **BN-2** is slightly bent with a bending angle of 11° (Figure 2a and 2b). In the N_2C_4 ring, the C–N bonds (1.39–1.41 Å) are shorter than the C–N single bonds (1.44 Å) between the backbone and the pendant groups, and the C=C bonds (1.41–1.44 Å) are longer than the ideal aromatic C=C bonds (1.38 Å),[13] demonstrating the 8π antiaromatic character (Figure 2c and 2d). Similarly, the 4π antiaromaticity of the B_2C_4 ring is supported by the shorter C–B bond lengths (1.55 Å) compared with the C–B single bonds (1.58 Å) between the backbone and the pendant groups, as well as the longer C=C bond lengths (1.43–1.46 Å) than the localized C=C bonds (1.38 Å).

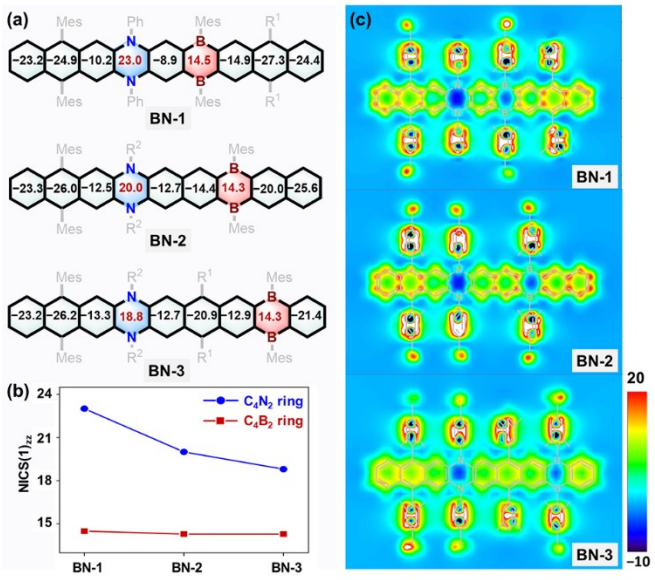

Figure 3. (a) DFT-calculated NICS(1)$_{zz}$ values. (b) Comparison of the NICS(1)$_{zz}$ values of the N_2C_4 and B_2C_4 rings in **BN-1**, **BN-2**, and **BN-3**. (c) 2D-ICSS maps of the three compounds at 1 Å above the XY plane.

Density functional theory (DFT) calculations were performed to analyze the antiaromaticity of the boron- and nitrogen-embedded hexagons. The calculated nucleus-independent chemical shift (NICS) values reveal that both the N_2C_4 and B_2C_4 rings are antiaromatic while other benzene rings are aromatic (Figure 3a). As increasing the distance between the N_2C_4 and B_2C_4 rings from **BN-1** to **BN-2** and **BN-3**, the antiaromaticity of the N_2C_4 rings is gradually decreased with NICS values changing from 23.0 to 20.0 and 18.8, whereas the B_2C_4 rings show similar antiaromaticity with nearly the same NICS values of 14.3–14.5 (Figure 3b). The decreased antiaromaticity of the N_2C_4 rings is attributed to the enhanced π-delocalization to the neighboring benzene rings.[14] Moreover, the de-shielded chemical environment (blue regions) in the isotropic chemical shielding surface (ICSS) maps and the anticlockwise current flow in the anisotropy of the induced current density (ACID) plots also support the antiaromatic character of the N_2C_4 and B_2C_4 rings in BN-doped nonacenes (Figure 3c and Figure S10).

The photophysical properties of these three compounds were then characterized. **BN-1** exhibits a vibronic absorption band with the absorption maximum (λ_{abs}) at 450 nm, and a blue-shifted absorption is observed for **BN-2** with λ_{abs} at 441 nm. By contrast, **BN-3** shows quite a different absorption feature with λ_{abs} at 474 and 509 nm (Figure 4a and Table S2). The optical gaps of **BN-1**, **BN-2**, and **BN-3** are 2.16, 2.41, and 2.35 eV, respectively, which are comparable to the electrochemical HOMO-LUMO gaps (2.29–2.39 eV). Time-dependent (TD) DFT calculations reveal that the $S_0 \rightarrow S_1$ excitation of the three compounds is attributed to the HOMO→LUMO transition, and the oscillator strengths (f) are 0.034 for **BN-1**, 0.023 for **BN-2**, and 0.145 for **BN-3** (Table S3–S5). The low f values of **BN-1** and **BN-2** are responsible for the absorption tails in the long-wavelength region (Figure S7–S9). On the other hand, **BN-1** exhibits red fluorescence with the emission maximum (λ_{em}) at 621 nm, while **BN-2** and **BN-3** show blue-shifted emission bands peaking at 601 and 553 nm, respectively. The Φ_F is determined to be 51% for **BN-1** and 56% for **BN-2**. Particularly, **BN-3** is strongly emissive with a high Φ_F of 92%. To shed light on the difference, transient photoluminescence spectra of the three compounds were recorded. The fluorescence lifetimes (τ) of **BN-1**, **BN-2**, and **BN-3** are measured to be 29.8, 21.2, and 7.3 ns, respectively (Figure 4c). The experimentally determined radiative rates (k_r) of **BN-1** and **BN-2** are similar (1.7×10^7 s^{-1} for **BN-1**; 2.6×10^7 s^{-1} for **BN-2**), whereas the k_r of **BN-3** is almost one order of magnitude higher (1.3×10^8 s^{-1}). Moreover, the nonradiative rates (k_{nr}) are 1.6×10^7 s^{-1} for **BN-1**, 2.0×10^7 s^{-1} for **BN-2**, and 1.1×10^7 s^{-1} for **BN-3**, which are at the same level (Figure 4d). Therefore, the large k_r of **BN-3** is the determining factor for its high Φ_F.

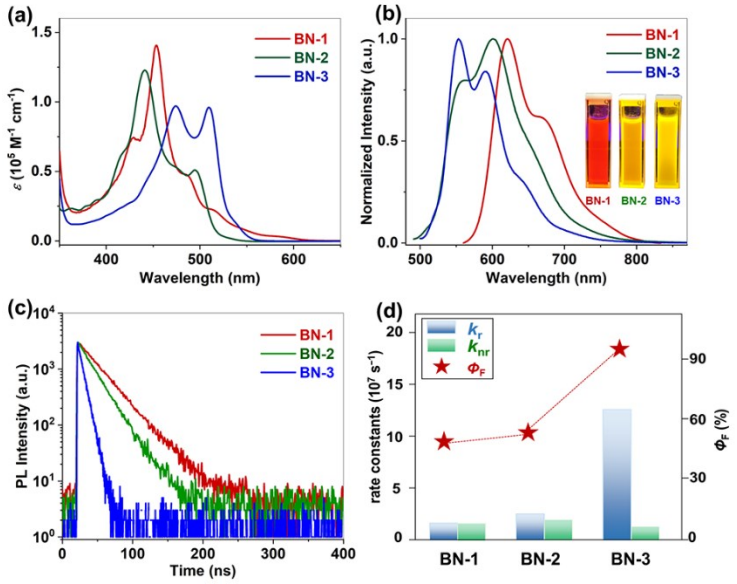

Figure 4. (a) UV-vis absorption spectra ($c = 1.0 \times 10^{-5}$), (b) normalized emission spectra ($c = 1.0 \times 10^{-6}$), and (c) transient photoluminescence decay curves of BN-doped nonacenes in toluene solutions. (d) Comparison of the k_r, k_{nr}, and Φ_F of **BN-1**, **BN-2**, and **BN-3**. Inset: photographs of **BN-1**, **BN-2**, and **BN-3** in toluene solutions under 365 nm UV light.

TDDFT-calculations in the S_1 excited state were then performed to give deeper insights into the luminescent properties of BN-doped nonacenes. The molecular orbitals and the energy diagrams of the monocyclic N_2C_4 and B_2C_4 rings and the BN-doped nonacenes are illustrated in Figure 5. The HOMO of BN-nonacenes is localized at the electron-rich nitrogen side of the backbone, while the LUMO is at the electron-deficient boron side. **BN-1**, **BN-2**, and **BN-3** exhibit similar LUMO distributions, which are determined by the LUMO of the monocyclic B_2C_4 ring. The LUMO levels of the three BN-nonacenes are almost the same, which is in accordance with the similar antiaromaticity of the B_2C_4 rings in these three compounds. On the other hand, **BN-1** and **BN-2** display similar HOMO distributions, which are dominated by the HOMO of the monocyclic N_2C_4 ring. The HOMO level of **BN-2** is lowered compared with that of **BN-1**, which could be explained by the decreased antiaromaticity of the N_2C_4 ring.[15] As the antiaromaticity of the N_2C_4 ring is further decreased in **BN-3**, the energy of the molecular orbital, which keeps the same pattern as the HOMO of **BN-1** and **BN-2**, is

significantly lowered, and an inversion between the HOMO and HOMO-1 patterns of **BN-1**/**BN-2** is observed in **BN-3**. The new molecular orbital arrangement in **BN-3** leads to a larger HOMO-LUMO overlap, which is also evidenced by the hole/electron distribution during the $S_1 \rightarrow S_0$ transition (Figure S11). This feature facilities a significantly higher *f* value of 0.240 for **BN-3** (0.026 for **BN-1** and 0.017 for **BN-2**) (Table S6–S8), which leads to a larger k_r and thus a higher Φ_F.[16]

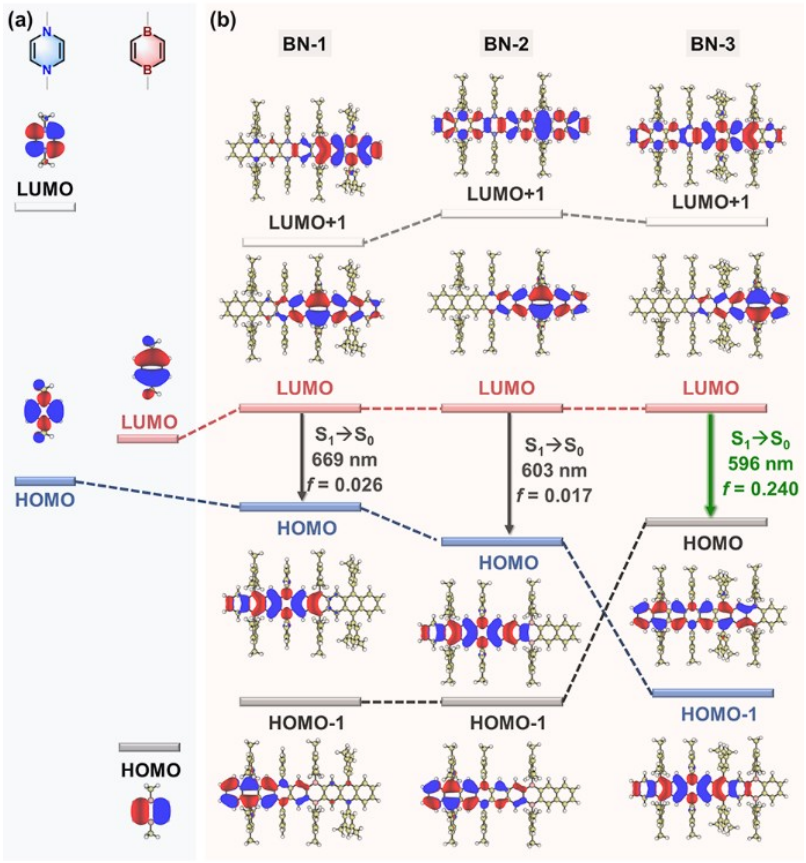

Figure 5. TDDFT-calculated molecular orbitals and energy diagrams of (a) the monocyclic N_2C_4 and B_2C_4 rings and (b) BN-doped nonacenes **BN-1**, **BN-2**, and **BN-3** in the S_1 excited state at the B3LYP/6-31G(d) level. *f* values represent the oscillator strength.

In summary, we have synthesized the hitherto longest BN-isosteres of nonacene **BN-1**, **BN-2**, and **BN-3** embedded with 4π antiaromatic B_2C_4 and 8π antiaromatic N_2C_4 heterocycles. Photophysical characterizations and theoretical calculations reveal that varying the doping position of the B_2C_4 and N_2C_4 rings remarkably affect the local

antiaromaticity and the molecular orbital arrangement, resulting in a favorable radiative transition and thus a high Φ_F of 92% for **BN-3**. From the synthetic point of view, the nonacene BN-isoseteres reported in this work greatly expand the length limit of BN-heteroacenes. Furthermore, the antiaromatic BN-doping mode provides a new design concept to enrich the chemistry of BN-doped PAHs and to modulate physical properties by molecular orbital engineering, thus offering new opportunities in the future development of BN-embedded conjugated materials.

Acknowledgements

We are grateful to the financial support from the National Natural Science Foundation of China (Nos. 22071120, 92256304, and 22221002), the National Key R&D Program of China (2020YFA0711500), the Open Fund of the State Key Laboratory of Luminescent Materials and Devices (South China University of Technology), and the Fundamental Research Funds for the Central Universities. The authors cordially thank Dr. Haibin Song and Mr. Hua Rong (College of Chemistry, Nankai University) for single-crystal X-ray structural analysis.

Keywords: acene • boron-nitrogen • antiaromaticity • isoelectronic analogues • luminescence

References

[1] a) J. E. Anthony, *Chem. Rev.* **2006**, *106*, 5028−5048; b) J. E. Anthony, *Angew. Chem. Int. Ed.* **2008**, *47*, 452–483; c) W. Chen, F. Yu, Q. Xu, G. Zhou, Q. Zhang, *Adv. Sci.* **2020**, *7*, 1903766; d) Q. Ye, C. Chi, *Chem. Mater.* **2014**, *26*, 4046–4056; e) M. Watanabe, Y. J. Chang, S.-W. Liu, T.-H. Chao, K. Goto, M. M. Islam, C.-H. Yuan, Y.-T. Tao, T. Shinmyozu, T. J. Chow, *Nat. Chem.* **2012**, *4*, 574–578.

[2] a) W. Zeng, J. Wu, *Chem* **2021**, *7*, 358–386; b) M. Müller, L. Ahrens, V. Brosius, J. Freudenberg, U. H. F. Bunz, *J. Mater. Chem. C* **2019**, *7*, 14011–14034.

[3] a) C. Tönshoff, H. F. Bettinger, *Chem. Eur. J.* **2021**, *27*, 3193–3212; b) R. Zuzak, R. Dorel, M. Kolmer, M. Szymonski, S. Godlewski, A. M. Echavarren, *Angew. Chem. Int. Ed.* **2018**, *57*, 10500–10505; c) B. Shen, J. Tatchen, E. Sanchez-Garcia, H. F. Bettinger, *Angew. Chem. Int. Ed.* **2018**, *57*, 10506–10509; d) A. Jancarik, J. Holec, Y. Nagata, M. Samal, A. Gourdon, *Nat. Commun.* **2022**, *13*, 223; e) K. Eimre, J. I. Urgel, H. Hayashi, M. Di Giovannantonio, P. Ruffieux, O. Gröning, H. Yamada, R. Fasel, C. A. Pignedoli, S. Sato, S. Otomo, Y. S. Chan, N. Aratani, D. Passerone, *Nat. Commun.* **2022**, *13*, 511; f) F. Eisenhut, T. Kühne, F. García, S. Fernández, E. Guitián, D. Pérez, G. Trinquier, G. Cuniberti, C. Joachim, D. Peña, F. Moresco, *ACS Nano* **2020**, *14*, 1011–1017; g) J. I. Urgel, S. Mishra, H. Hayashi, J. Wilhelm, C. A. Pignedoli, M. Di Giovannantonio, R. Widmer, M. Yamashita, N. Hieda, P. Ruffieux, H. Yamada, R. Fasel, *Nat. Commun.* **2019**, *10*, 861.

[4] T. Kitao, T. Miura, R. Nakayama, Y. Tsutsui, Y. S. Chan, H. Hayashi, H. Yamada, S. Seki, T. Hitosugi, T. Uemura, *Nat. Synth.* **2023**, *2*, 848–854.

[5] a) N. Zeitter, N. Hippchen, A. Weidlich, P. Jäger, P. Ludwig, F. Rominger, A. Dreuw, J. Freudenberg, U. H. F. Bunz, *Chem. Eur. J.* **2023**, doi: 10.1002/chem.202302323; b) N. Zeitter, N. Hippchen, S. Maier, F. Rominger, A. Dreuw, J. Freudenberg, U. H. F. Bunz, *Angew. Chem. Int. Ed.* **2022**, *61*, e202200918; c) I. Kaur, M. Jazdzyk, N. N. Stein, P. Prusevich, G. P. Miller, *J. Am. Chem. Soc.* **2010**, *132*, 1261-1263; d) B. Purushothaman, M. Bruzek, S. R. Parkin, A.-F. Miller, J. E. Anthony, *Angew. Chem. Int. Ed.* **2011**, *50*, 7013-7017.

[6] a) A. Borissov, Y. K. Maurya, L. Moshniaha, W.-S. Wong, M. Żyła-Karwowska, M. Stępień, *Chem. Rev.* **2022**, *122*, 565–788; b) Y. Guo, C. Chen, X.-Y. Wang, *Chin. J. Chem.* **2023**, *41*, 1355–1373; c) M. Stępień, E. b. Gońka, M. Żyła, N. Sprutta, *Chem. Rev.* **2017**, *117*, 3479–3716.

[7] a) T. Jin, L. Kunze, S. Breimaier, M. Bolte, H.-W. Lerner, F. Jäkle, R. F. Winter, M. Braun, J.-M. Mewes, M. Wagner, *J. Am. Chem. Soc.* **2022**, *144*, 13704–13716; b) Z. Zhang, Q. Zhang, *Mater. Chem. Front.* **2020**, *4*, 3419–3432; c) U. H. F. Bunz, J. Freudenberg, *Acc. Chem. Res.* **2019**, *52*, 1575–1587; d) M. Chu, J.-X. Fan, S. Yang, D.

Liu, C. F. Ng, H. Dong, A.-M. Ren, Q. Miao, *Adv. Mater.* **2018**, *30*, 1803467; e) J. Li, Q. Zhang, *ACS Appl. Mater. Interfaces* **2015**, *7*, 28049–28062; f) E. von Grotthuss, A. John, T. Kaese, M. Wagner, *Asian J. Org. Chem.* **2018**, *7*, 37–53.

[8] a) S. Dong, T. Y. Gopalakrishna, Y. Han, H. Phan, T. Tao, Y. Ni, G. Liu, C. Chi, *J. Am. Chem. Soc.* **2019**, *141*, 62–66; b) Y. Wang, S. Qiu, S. Xie, L. Zhou, Y. Hong, J. Chang, J. Wu, Z. Zeng, *J. Am. Chem. Soc.* **2019**, *141*, 2169–2176; c) Y. Chen, H. Kueh, T. Y. Gopalakrishna, S. Dong, Y. Han, C. Chi, *Org. Lett.* **2019**, *21*, 3127–3130; d) M. Dietz, M. Arrowsmith, K. Drepper, A. Gärtner, I. Krummenacher, R. Bertermann, M. Finze, H. Braunschweig, *J. Am. Chem. Soc.* **2023**, *145*, 15001–15015; e) J. E. Barker, A. D. Obi, D. A. Dickie, R. J. Gilliard, Jr., *J. Am. Chem. Soc.* **2023**, *145*, 2028–2034; f) C. Chen, M.-W. Wang, X.-Y. Zhao, S. Yang, X.-Y. Chen, X.-Y. Wang, *Angew. Chem. Int. Ed.* **2022**, *61*, e202200779.

[9] a) P. G. Campbell, A. J. V. Marwitz, S.-Y. Liu, *Angew. Chem. Int. Ed.* **2012**, *51*, 6074–6092; b) S. A. Iqbal, J. Pahl, K. Yuan, M. J. Ingleson, *Chem. Soc. Rev.* **2020**, *49*, 4564–4591; c) Z. X. Giustra, S.-Y. Liu, *J. Am. Chem. Soc.* **2018**, *140*, 1184–1194; d) X.-Y. Wang, J.-Y. Wang, J. Pei, *Chem. Eur. J.* **2015**, *21*, 3528–3539; e) Y. Yu, L. Wang, D. Lin, S. Rana, K. S. Mali, H. Ling, L. Xie, S. De Feyter, J. Liu, *Angew. Chem. Int. Ed.* **2023**, *62*, e202303335; f) J.-J. Zhang, L. Yang, F. Liu, Y. Fu, J. Liu, A. A. Popov, J. Ma, X. Feng, *Angew. Chem. Int. Ed.* **2021**, *60*, 25695–25700; g) J. Wang, A. Zheng, Y. Xiang, J. Liu, *J. Am. Chem. Soc.* **2023**, *145*, 14912–14921; h) M. Vanga, A. Sahoo, R. A. Lalancette, F. Jäkle, *Angew. Chem. Int. Ed.* **2022**, *61*, e202113075; i) K. Liu, Z. Jiang, R. A. Lalancette, X. Tang, F. Jäkle, *J. Am. Chem. Soc.* **2022**, *144*, 18908–18917; j) Z. Chang, C. Chen, X.-Y. Wang, *Chem. Lett.* **2023**, *52*, 586–597; k) C. Chen, C.-Z. Du, X.-Y. Wang, *Adv. Sci.* **2022**, *9*, 2200707; l) K. Zhao, Z. F. Yao, Z. Y. Wang, J. C. Zeng, L. Ding, M. Xiong, J. Y. Wang, J. Pei, *J. Am. Chem. Soc.* **2022**, *144*, 3091–3098; m) P. F. Zhang, J. C. Zeng, F. D. Zhuang, K. X. Zhao, Z. H. Sun, Z. F. Yao, Y. Lu, X. Y. Wang, J. Y. Wang, J. Pei, *Angew. Chem. Int. Ed.* **2021**, *60*, 23313–23319.

[10]a) S. Jeong, E. Park, J. Kim, S. B. Park, S. H. Kim, W. Choe, J. Kim, Y. S. Park, *Angew. Chem. Int. Ed.* **2023**, doi: 10.1002/anie.202314148; b) W. Li, C.-Z. Du, X.-Y.

Chen, L. Fu, R.-R. Gao, Z.-F. Yao, J.-Y. Wang, W. Hu, J. Pei, X.-Y. Wang, *Angew. Chem. Int. Ed.* **2022**, *61*, e202201464; c) L. Palomino-Ruiz, S. Rodríguez-González, J. G. Fallaque, I. R. Márquez, N. Agraït, C. Díaz, E. Leary, J. M. Cuerva, A. G. Campaña, F. Martín, A. Millán, M. T. González, *Angew. Chem. Int. Ed.* **2021**, *60*, 6609–6616; d) S. Kawai, S. Nakatsuka, T. Hatakeyama, R. Pawlak, T. Meier, J. Tracey, E. Meyer, A. S. Foster, *Sci. Adv.* **2018**, *4*, eaar7181.

[11] a) T. Agou, J. Kobayashi, T. Kawashima, *Org. Lett.* **2006**, *8*, 2241–2244; b) S. M. Suresh, E. Duda, D. Hall, Z. Yao, S. Bagnich, A. M. Z. Slawin, H. Bässler, D. Beljonne, M. Buck, Y. Olivier, A. Köhler, E. Zysman-Colman, *J. Am. Chem. Soc.* **2020**, *142*, 6588–6599; c) M. Metzler, A. Virovets, H.-W. Lerner, M. Wagner, *J. Am. Chem. Soc.* **2023**, doi: 10.1021/jacs.3c09029.

[12] Deposition Numbers 2304085 (**BN-1**) and 2304089 (**BN-2**) contain the supplementary crystallographic data for this paper. These data are provided free of charge by the joint Cambridge Crystallographic Data Centre and Fachinformationszentrum Karlsruhe Access Structures service.

[13] F. H. Allen, O. Kennard, D. G. Watson, L. Brammer, A. G. Orpen, R. Taylor, *J. Chem. Soc., Perkin Trans. 2* **1987**, S1–S19.

[14] R. Kotani, L. Liu, P. Kumar, H. Kuramochi, T. Tahara, P. Liu, A. Osuka, P. B. Karadakov, S. Saito, *J. Am. Chem. Soc.* **2020**, *142*, 14985–14992.

[15] S.-J. Jhang, J. Pandidurai, C.-P. Chu, H. Miyoshi, Y. Takahara, M. Miki, H. Sotome, H. Miyasaka, S. Chatterjee, R. Ozawa, Y. Ie, I. Hisaki, C.-L. Tsai, Y.-J. Cheng, Y. Tobe, *J. Am. Chem. Soc.* **2023**, *145*, 4716–4729.

[16] R. C. Hilborn, *Am, J. Phys* **1982**, *50*, 982–986.